Heme Oxygenase (HO-1): His-132 Stabilizes a Distal Water Ligand and Assists Catalysis†

Angela Wilks,‡ Paul R. Ortiz de Montellano,*,‡ Jie Sun,§ and Thomas M. Loehr§

Department of Pharmaceutical Chemistry, School of Pharmacy, and Liver Center, University of California, San Francisco, California 94143-0446, and Department of Chemistry, Biochemistry, and Molecular Biology, Oregon Graduate Institute of Science and Technology, P.O. Box 91000, Portland, Oregon 97291-1000

Received October 6, 1995; Revised Manuscript Received November 7, 1995⊗

ABSTRACT: His-25 and His-132 are the primary candidates for the proximal heme iron ligand in heme oxygenase isozyme-1 (HO-1). The unambiguous spectroscopic demonstration that His-25 is the proximal iron ligand leaves the role of His-132 uncertain. Absorption and resonance Raman spectroscopy are used here to establish that mutation of His-132 to an alanine, glycine, or serine does not alter the histidine−iron bond, but results in the loss of the water molecule coordinated to the distal side of the iron in the wild-type enzyme−substrate complex. The His-132 mutations also (a) destabilize the ferrous−O_2 complex with respect to autoxidation, which should result in partial uncoupling of NADPH consumption from heme oxidation, and (b) decrease the affinity of the enzyme for heme. The catalytic activity of the protein is decreased but not suppressed by these mutations: the H132G and H132A mutants retain 40−50% and the H132S mutant 20% of the activity of the wild-type protein. His-132, however, is required for catalytic turnover of the protein with H_2O_2. These results place His-132 close to the iron on the distal side of the heme pocket and indicate that His-132 facilitates, but is not absolutely required for, the catalytic turnover of HO-1.

Heme oxygenase, the enzyme that oxidizes heme to biliverdin and CO, is known to exist in two forms (Maines et al., 1986; Maines, 1992a). One form, commonly known as HO-1,[1] is induced by both a variety of chemical agents and a range of stress conditions and is found in highest concentrations in the spleen and liver (Maines et al., 1986; Maines, 1992a). The second form, known as HO-2, is not inducible and is found in highest concentrations in the brain and testes. The biological activities of biliverdin and CO, the two products of the reaction (Figure 1), make heme oxygenase of considerable physiological interest. Excretion of bilirubin, the reduction product of biliverdin, is impaired in many newborn children and in individuals with a genetic deficiency of glucuronyl transferase (Maines, 1992b). Unconjugated bilirubin is neurotoxic, and interventions that prevent its accumulation, including the inhibition of heme oxygenase, are of potential clinical importance. Carbon monoxide, the second product of the heme oxygenase reaction, may also be of physiological importance. Recent studies have provided evidence that CO, for which heme oxygenase is the only physiological source in mammals, may function as a neurotransmitter akin to nitric oxide (Verma et al., 1993; Stevens & Wang, 1993; Marks, 1994). HO-2, the noninducible isoform located primarily in the brain, may therefore play an important role in biological signaling processes.

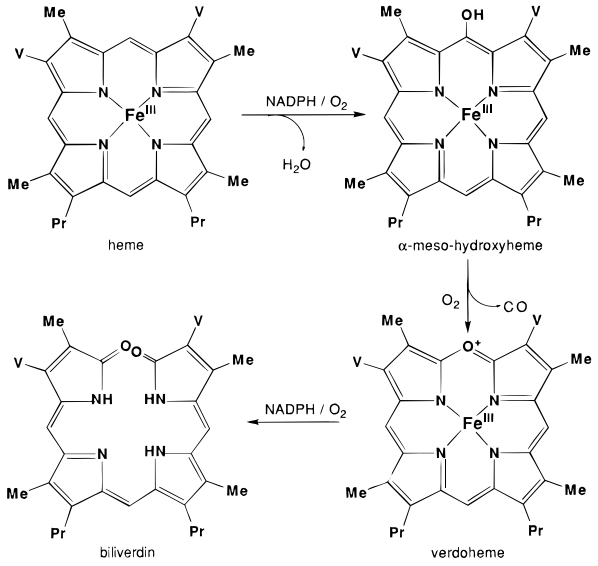

FIGURE 1: Reaction intermediates in the heme oxygenase-catalyzed oxidation of heme to biliverdin. The substituents on the porphyrin are vinyl (V) and propionate (Pr).

Human heme oxygenase is a 32 kDa protein with a C-terminal lipophilic domain that anchors it to the endoplastic reticulum (Yoshida et al., 1988). We have demonstrated that a truncated protein lacking the 23 C-terminal amino acids that make up the membrane anchor can be expressed in *Escherichia coli* in high yield. The truncated protein is soluble rather than membrane-bound and retains full catalytic activity (Wilks & Ortiz de Montellano, 1993). A protein lacking the 26 C-terminal amino acids and in which the last two amino acids have been mutated (S262R, S263L) has been expressed independently and shown to be soluble and

† This work was supported by Grants DK30297, 5 P30 DK26743, and GM34468 from the National Institutes of Health.

* Author to whom correspondence should be addressed.

‡ University of California.

§ Oregon Graduate Institute of Science and Technology.

⊗ Abstract published in *Advance ACS Abstracts,* January 1, 1996.

[1] Abbreviations: heme, iron protoporphyrin IX regardless of the oxidation and ligation states of the iron; HO-1, heme oxygenase isozyme-1; hHO-1, truncated human HO-1; WT, wild-type; HPLC, high-pressure liquid chromatography; rRaman, resonance Raman.

0006-2960/96/0435-930$12.00/0

to retain only part of the catalytic activity (Ishikawa et al., 1992). Alignment of the available heme oxygenase sequences identified four conserved histidine residues. Mutagenesis experiments have shown that catalytic activity is completely (>99%) lost when two of these residues, His-25 and His-132, are mutated to alanines. Mutation of the other two conserved histidines did not alter the catalytic activity (Ishikawa et al., 1992). Subsequent work confirmed that the H25A HO-1 mutant is catalytically inactive and demonstrated, by means of absorption, resonance Raman, and EPR spectroscopies, that His-25 is, in fact, the proximal iron ligand (Sun et al., 1993, 1994; Takahashi et al., 1994a,b). Identification of His-25 as the proximal ligand is strengthened by the demonstration that the addition of exogenous imidazole to the H25A HO-1 mutant restores both the histidine coordination to the iron and the full catalytic activity of the mutant protein (Wilks et al., 1995b).

The role of His-132 in HO-1 is unclear in view of the unambiguous evidence that His-25 is the proximal iron ligand in that protein. McCoubrey and Maines (1993) have reported that the H151A HO-2 mutant is inactive and proposed that His-151 is the iron ligand in that form of the enzyme. On the basis of this finding and the high degree of sequence conservation, they proposed that the corresponding histidine (His-132) should be the iron ligand in HO-1. This possibility is ruled out by the recent data, but the role of His-132, which is located within the most highly conserved region of the protein, remains obscure. The report by Ishikawa et al. (1992) that the H132A HO-1 mutant is only 1% as active as the wild-type enzyme is consistent with the reported inactivity of the H151A HO-2 mutant. However, reexamination of the H132A HO-1 mutant showed that it actually retains nearly complete catalytic activity (Ito-Maki et al., 1995). The protein used in the latter study appears, from the SDS−PAGE analysis given in the paper, to have been almost completely digested to a 28 kDa fragment. Earlier work showed that the 28 kDa proteolytic fragment of native HO-1 does not turn over catalytically with cytochrome P450 reductase and NADPH, but does oxidize the heme to biliverdin under coupled oxidation conditions (i.e., with ascorbic acid) (Yoshida et al., 1991). Coupled oxidation produces biliverdin from free iron porphyrins, hemoglobin, and a variety of other hemoproteins, and therefore is a relatively nonspecific process (Bonnett & McDonagh, 1973; Docherty & Brown, 1984). The catalytic activity reported for the 28 kDa fragment of the H132A HO-1 mutant is therefore difficult to evaluate (Ito-Maki et al., 1995). Furthermore, direct spectroscopic evidence that the proteins fold and bind heme in a normal fashion is not available for either the H132A HO-1 mutant or the H151A HO-2 mutant.

We report here the characterization of the H132A, H132G, and H132S HO-1 mutants by UV−vis and resonance Raman spectroscopy and the determination of the catalytic activities of the proteins. The results confirm, as expected, that His-132 is not the axial ligand to the iron. More importantly, they establish that His-132 plays a critical role in the coordination of a water molecule to the distal site of the iron atom. The finding that the His-132 mutants retain partial catalytic activity establishes, furthermore, that His-132 facilitates but is not essential for catalytic turnover.

EXPERIMENTAL PROCEDURES

General Methods. The HO-1 construct used for these experiments coded for the human liver protein minus the 23 C-terminal amino acids (Wilks et al., 1995a). The human truncated protein is designated here as hHO-1. Plasmid purification, sequencing, subcloning, and bacterial transformations were carried out by standard procedures (Sambrook et al., 1989). Heterologously expressed rat NADPH−cytochrome P450 reductase was a kind gift from Bettie Sue Masters (University of Texas Health Science Center, San Antonio). Deionized, doubly distilled water was used for all biochemical experiments. Oligonucleotide synthesis was carried out at the University of California at San Francisco Biomolecular Resource Center using an Applied Biosystems 380B DNA synthesizer. HPLC was done on a Hewlett-Packard Series II 1090 liquid chromatography instrument.

Bacterial Strain. *Escherichia coli* strain DH5α[F′,*ara*Δ-(*lac-proAB*)rpsL*ϕ80dlacZ*ΔM15*hsd*R17] was used for the expression of heme oxygenase.

Mutagenesis. Site-specific mutagenesis was carried out using the Altered Sites II mutagenesis kit (Promega, Madison, WI). Antibiotic selection (ampicillin) was used to obtain a high frequency of mutants. Transformants were screened by restriction digestion and were confirmed by sequencing.

Expression, Purification, and Characterization of the Heme Oxygenase Mutants. The His-132 hHO-1 mutants were expressed and purified as previously described for the wild-type proteins (Wilks & Ortiz de Montellano, 1993; Wilks et al., 1995a). The heme oxygenase activity was measured, and the biliverdin products were analyzed by HPLC as previously described (Wilks & Ortiz de Montellano, 1993).

Purification and Characterization of the Heme Complexes with the His-132 hHO-1 Mutants. The His-132 hHO-1−heme complexes were purified as previously described for the wild-type protein (Wilks & Ortiz de Montellano, 1993). The spectra of the complexes in 100 mM potassium phosphate buffer (pH 7.4) were recorded on a Hewlett-Packard 8450A spectrophotometer. The ferrous−CO complex was formed by adding sodium dithionite to a CO-saturated solution of the complexes of the ferric His-132 hHO-1 mutants. The ferrous−O_2 complex was obtained by passing the CO complex through a Sephadex G-25 column preequilibrated with 10 mM potassium phosphate (pH 7.4) buffer.

Reaction of the Heme−His-132 hHO-1 Mutant Complexes with Peroxides. One equivalent of 8 mM H_2O_2 (1 μL) in 0.1 M potassium phosphate (pH 7.4) buffer was added to a solution of the His-132 hHO-1 complexes (8 μM) in the same buffer. The loss of the Soret absorbance was monitored, and when maximum loss was observed, pyridine was added to the solution at a final concentration of 20%.

Reactions of the His-132 hHO-1 Mutant−Heme Complexes with Cytochrome P450 Reductase and NADPH. Cytochrome P450 reductase (25 μM, 3:1 reductase to heme oxygenase) and NADPH (10 mM) were added to cuvettes containing CO-presaturated solutions of the His-132 hHO-1 mutant−heme complexes (8.5 μM) in 0.1 M potassium phosphate buffer (pH 7.4). The progress of the reactions was monitored by UV spectroscopy. After 10 min, at which time no further changes in the spectra were observed, the

Table 1: Yields and Kinetic Parameters for the H132G, H132A, and H132S Mutants

protein	purified yield (mg L^{-1} of cells)	K_m(heme) (μM)	V_{max} (nmol h^{-1} $nmol^{-1}$)	K_d(heme) (μM)
wild-type	30−35	3 ± 1.6	44 ± 1.5	0.84 ± 0.2
H132G	4−5	14 ± 3	22 ± 1.1	28 ± 3
H132A	3−5	14 ± 7	18 ± 2.1	11 ± 2
H132S	5	18 ± 8	8.3 ± 0.6	46 ± 4

biliverdin products were extracted for HPLC analysis as previously described (Wilks & Ortiz de Montellano, 1993).

Measurement of the Kinetic Parameters for the Heme Oxygenase Mutants. The K_m and V_{max} values were obtained from application of the Michaelis−Menten equation to the data obtained from the standard assay procedure (Yoshida & Kikuchi, 1979), in which the heme concentration was varied between 5 and 100 μM. The K_d value was obtained from the absorbance difference at 400−350 nm upon the addition of heme increments to the apoprotein.

Resonance Raman Studies. The ferric heme−hHO-1 complexes were examined at a concentration of ~60 μM in 100 mM potassium phosphate buffer (pH 7.4). To obtain the ferrous complexes, samples in septum-sealed capillary tubes were purged with argon gas for ~10 min, and then minimal amounts of freshly prepared 100 mM sodium dithionite solution were added. The reduction was monitored by UV−visible spectroscopy.

Resonance Raman spectra were obtained with a custom spectrometer consisting of a McPherson (Acton, MA) Model 2061/2067 single monochromator (1800 grooves/mm grating) operated at a focal length of 0.67 m and a Princeton Instruments (Trenton, NJ) LN1100 CCD detector. Rayleigh scattering was attenuated by use of Kaiser Optical (Ann Arbor, MI) notch or supernotch filters. Excitation sources were a Coherent (Santa Clara, CA) Innova 90-6 argon laser (514.5 nm), a Coherent Innova 302 krypton laser (413.1 nm), and a Liconix 4240NB He/Cd laser (441.6 nm). Incident powers were 12−20 mW for Soret excitation (413.1, 441.6 nm) and 30 mW for Q excitation (514.5 nm). Spectra were collected in a 90° scattering geometry from solution samples contained in capillary tubes in contact with a copper cold-finger immersed in an ice−water bath. Spectral resolution was ~5.0 cm^{-1}. CCl_4 was used as a standard for polarization, and indene was used as the calibrant for the Raman frequency shifts. Some spectra were subjected to correction by applying polynomial least-squares fits to the baselines using Galactic's (Salem, NH) GRAMS/386 software. Optical absorption spectra of the intact Raman samples were obtained on a Perkin-Elmer Lambda 9 spectrophotometer at a spectral bandwidth of 2 nm by placing the sample capillary tubes in a black Delrin cell holder (Loehr & Sanders-Loehr, 1993).

RESULTS

Expression and Purification of the His-132 hHO-1 Mutants. The protein yields for the three mutants are variable but are reduced relative to the yield of the wild-type protein (Table 1). SDS−PAGE analysis indicates that the recombinant proteins are highly purified and have the expected molecular weight (Figure 2). The H132A and H132G mutants retain 40−50%, and the H132S mutant only 20%, of the wild-type catalytic activity (Table 1). The K_m values for the oxidation of heme increase by a factor of ~5 in the

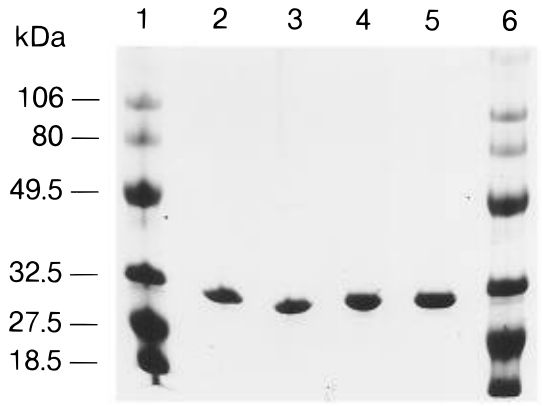

FIGURE 2: SDS−PAGE analysis of the H132G, H132A, and H132S hHO-1 mutants purified from the *E. coli* expression system: lanes 1 and 6, molecular mass markers; lane 2, WT hHO-1; lane 3, H132G hHO-1; lane 4, H132A hHO-1; lane 5, H132S hHO-1. The gel was stained with Coomassie Blue.

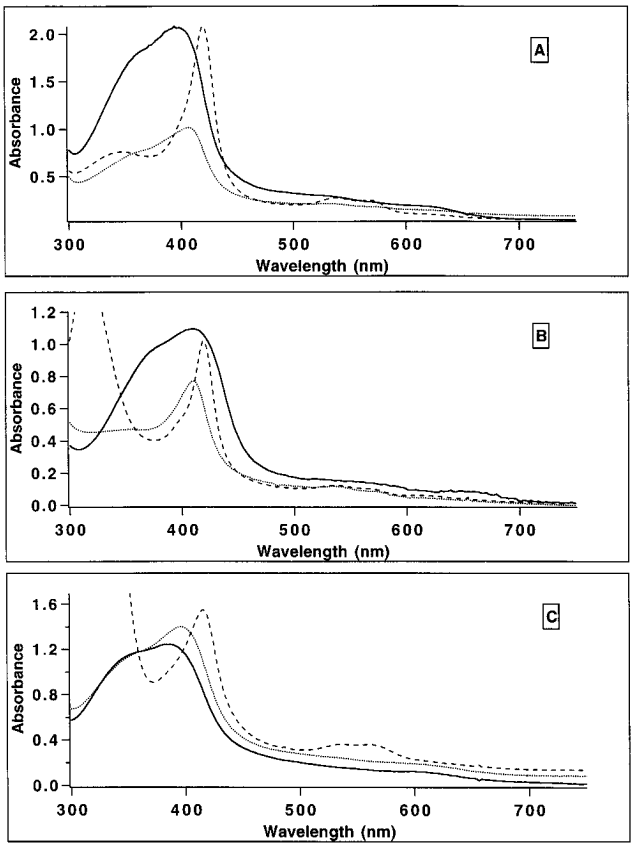

FIGURE 3: Absorption spectra of the complexes of heme with the (A) H132G, (B) H132A, and (C) H132S hHO-1 mutants. For each protein, the spectra of the ferric (—), ferrous−CO (- - -), and ferrous−O_2 complexes (•••) are shown. The last two spectra were obtained after passage of the sample through a Sephadex G25 column. The relative intensities of the absorption bands therefore are not necessarily proportional to each other.

His-132 mutants, although a much larger increase is seen in the spectroscopically determined heme dissociation constants (K_d) for the mutants relative to wild-type hHO-1 (Table 1).

Spectroscopic Properties of the His-132 hHO-1 Mutants. The ferric Soret absorbance of the heme−H132G hHO-1 complex is broader and is shifted from 404 to 394 nm with respect to the spectrum of the native protein (Figure 3A). Reduction with dithionite under an atmosphere of CO yields the ferrous−CO complex with a Soret maximum at 420 nm and well-defined α- and β-bands at 568 and 538 nm,

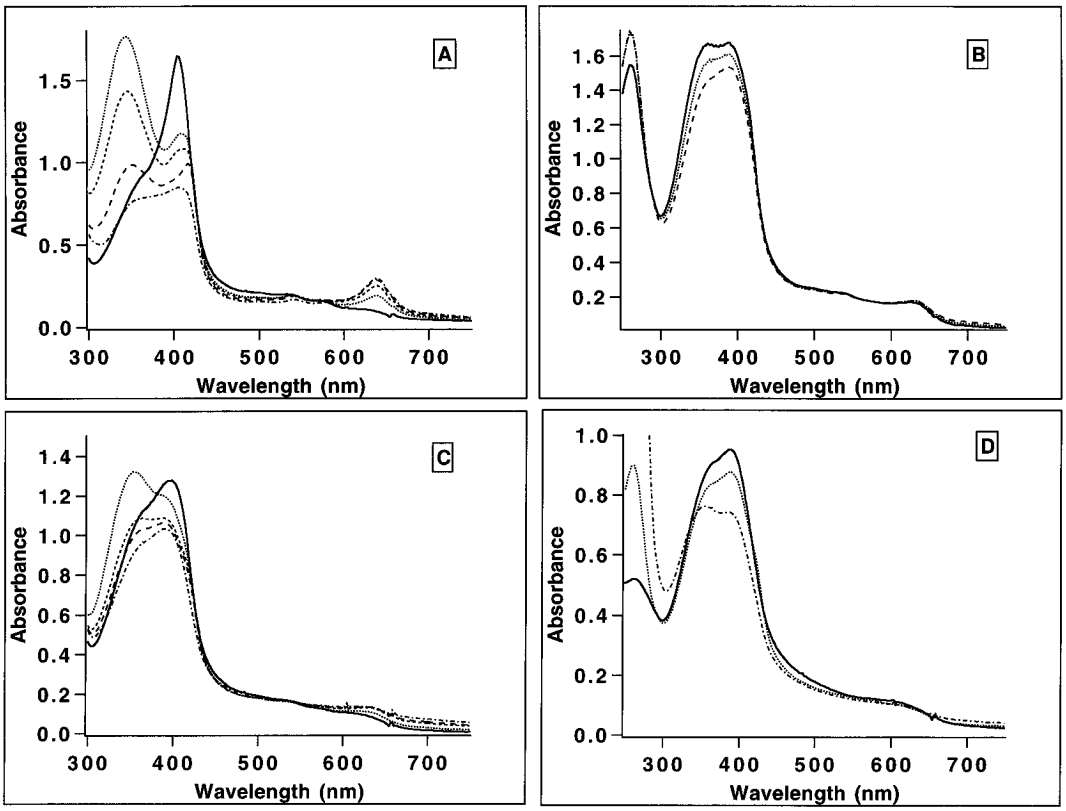

FIGURE 4: Spectral changes observed during normal catalytic turnover of heme complexes with (A) wild-type hHO-1, (B) H132G hHO-1, (C) H132A hHO-1, and (D) H132S hHO-1. For each protein, the spectra shown are of the resting ferric heme complex (—) and of the complex at the times indicated after the addition of NADPH: immediately (···), 5 min (- - -), 10 min (— —), and 20 min (— · —).

respectively, identical to those of the wild-type enzyme (Figure 3A). Passage of the CO complex through a Sephadex G-25 column causes the Soret band to shift from 420 to 410 nm and the α-/β-bands to shift to 574 and 540 nm (Figure 3A), respectively, as expected for conversion of the CO complex to the ferrous−O_2 complex during chromatography. Nearly identical spectra were obtained for the heme−H132A hHO-1 complex (Figure 3B).

The heme−H132S hHO-1 ferric Soret broadened and shifted to 386 nm (Figure 3C). Reduction and treatment with CO produce the ferrous−CO complex, with a Soret band at 415 nm and α- and β-bands at 560 and 536 nm, respectively (Figure 3C). In contrast to the other two mutants, passage of the ferrous−CO complex through Sephadex G-25 broadens the Soret band and shifts it to 396 nm with apparent loss of the α-β-bands (Figure 3C). This suggests that the enzyme reverts to the ferric state, although the absorption maximum is initially shifted by 10 nm from its position in the ferric enzyme. A spectrum closer to that of the ferric enzyme is obtained if the sample is allowed to stand for a period of time. The nature of the intermediate species is not known.

Catalytic Turnover of the His-132 hHO-1 Mutants. Addition of NADPH and cytochrome P450 reductase causes a decrease in the intensity without an apparent shift in the position of the Soret band of the ferric heme−H132G and H132A hHO-1 complexes (Figure 4B,C). In contrast, similar treatment of the wild-type heme−hHO-1 complex shifts the Soret maximum to 418 nm due to formation of the ferrous−CO complex, followed by a slower shift to 410 nm as the CO is replaced by O_2 (Figure 4A). In the presence of air, the wild-type heme−hHO-1 complex is converted to biliverdin, as indicated by the further loss of Soret absorbance and an increase in absorbance between 640 and 680 nm (Figure 4A). In contrast, little increase in absorbance in the 640−680 nm region is observed with the complexes of heme with H132G, H132A, or H132S hHO-1 (Figure 4B−D). In the case of wild-type hHO-1, extraction of the product followed by HPLC analysis indicates quantitative conversion of the heme to biliverdin IXα. No residual heme is observed. Extraction and HPLC of the products from the H132A and H132G hHO-1 incubations indicate that the heme is specifically converted to the biliverdin by oxidation of the heme at the α-*meso*-carbon. In the case of the heme−H132S hHO-1 complex, it has not been possible to identify the isomer of biliverdin that is formed due to the low yields of product.

Resonance Raman Characterization of the H132A hHO-1 Mutant. His-25 and His-132 are the only essential conserved histidines in heme oxygenase (Ishikawa et al., 1992). The resonance Raman spectra (low-frequency region) of ferrous heme complexes of the wild-type (WT), H132S, H132A, and H25A hHO-1 enzymes are shown in Figure 5. The spectrum of the WT species has a prominent band at 216 cm^{-1}. This band, which is sensitive to metal replacement and ^{54}Fe substitution, has been assigned to an Fe−N_{His} stretching vibration (Sun et al., 1993, 1994; Takahashi et al., 1994a,b). The proximal histidine ligation is also evident in the EPR spectrum (Sun et al., 1993; Takahashi et al., 1994a). We have previously identified the proximal histidine ligand to be His-25 (Sun et al., 1994), as the rRaman spectrum of H25A lacks the Fe−N_{His} stretching vibration (Figure 5). When His-132, the residue believed to be in the distal pocket, is mutated to an alanine or serine, the prominent Fe−N_{His} stretching band at 216 cm^{-1} remains (Figure 5), reinforcing

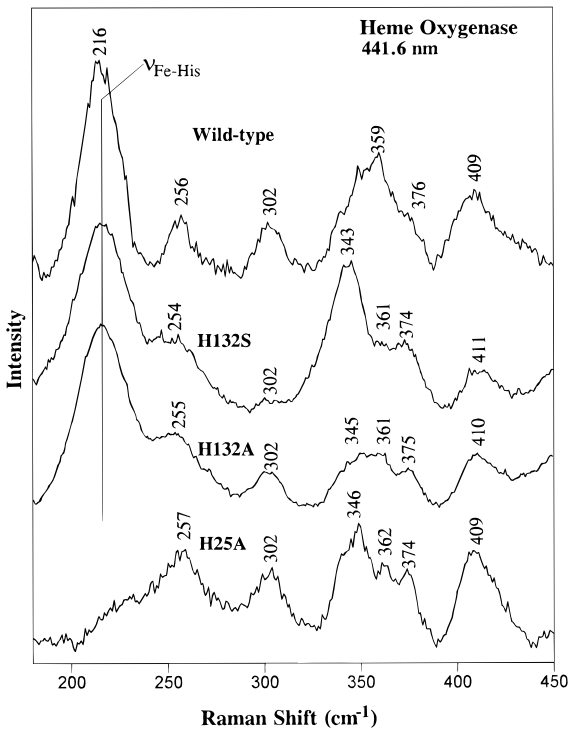

FIGURE 5: Resonance Raman spectra of ferrous heme complexes of wild-type, H132S, H132A, and H25A hHO-1 with 441.6 nm excitation.

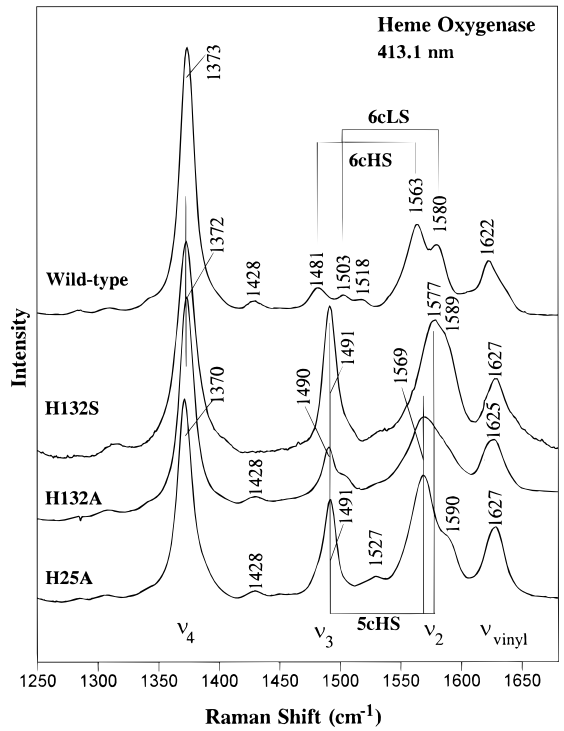

FIGURE 6: Resonance Raman spectra of the ferric heme complexes of wild-type, H132S, H132A, and H25A hHO-1 with 413.1 nm excitation. The bands indicative of 6-coordinate high-spin (6cHS), 6-coordinate low-spin (6cLS), and 5-coordinate high-spin (5cHS) complexes are shown.

our previous conclusion that His-25 is the proximal heme ligand.

The rRaman spectra of ferric heme complexes of the wild-type, H132S, H132A, and H25A hHO-1 enzymes obtained with 413.1 and 514.5 nm excitation are shown in Figures 6 and 7, respectively. The Raman bands in this spectral region

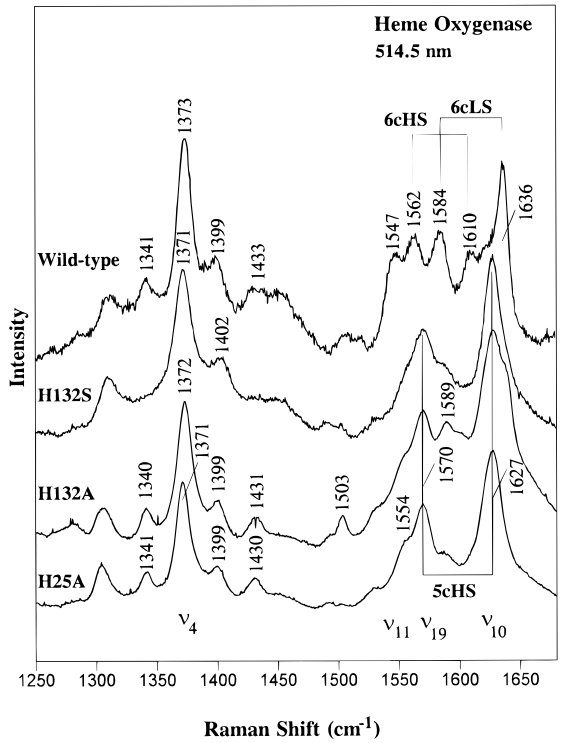

FIGURE 7: Resonance Raman spectra of ferric heme complexes of wild-type, H132S, H132A, and H25A hHO-1 with 514.5 nm excitation. The bands indicative of 6-coordinate high-spin (6cHS) and 6-coordinate low-spin (6cLS) complexes are shown.

(1250−1700 cm^{-1}) are from porphyrin skeletal vibrations. The strong band at ∼1372 cm^{-1} (ν_4) observed in these spectra is sensitive to the iron oxidation state and is typical for ferric hemes. A number of other Raman frequencies in this range (ν_2, ν_3, ν_{10}, ν_{19}) are known to be sensitive to the iron spin and ligation states and thus provide more detailed information about the heme environment. The rRaman spectra of the WT enzyme−substrate complex show a mixture of 6cHS and 6cLS heme Raman bands (Sun et al., 1993). The frequencies of porphyrin skeletal modes at 1563 (ν_2), 1481 (ν_3) (Figure 6), 1610 (ν_{10}), and 1562 cm^{-1} (ν_{19}) (Figure 7) are indicative of the presence of a 6cHS heme. The corresponding 6cLS heme bands are located at 1580 (ν_2), 1503 (ν_3) (Figure 6), 1636 (ν_{10}), and 1584 cm^{-1} (ν_{19}) (Figure 7). Previous studies concluded that the two axial heme ligands of the hexacoordinate species are a histidine and a H_2O (possibly OH^-) (Sun et al., 1993; Takahashi et al., 1994). The rRaman spectra of H25A have also been studied and are characteristic of a 5-coordinate high-spin heme (Sun et al., 1994). Since His-25 is the proximal heme ligand in the wild-type enzyme, the fifth ligand in H25A is an unidentified weak ligand $Fe^{III}-X$, where X may be H_2O. The rRaman spectra of H132S and H132A are also different from those of the wild-type enzyme (His25−Fe^{III}−H_2O) and are characteristic of 5 cHS ferric hemes[2] instead of 6cHS or 6cLS hemes. For H132S, these characteristic porphyrin skeletal bands are at 1577 (ν_2), 1491 (ν_3) (Figure 6), 1627

[2] In the rRaman spectra of the H132A mutant, a small peak at 1503 cm^{-1} is also seen. This peak probably originates from a 6cLS ferric heme. It is possible that a very small percentage of ferric heme−H132A hHO-1 complex exists as a species similar to the wild-type complex (His-25 and H_2O axial coordination). Some (ferric) heme proteins such as cytochrome *c* peroxidase also exhibit such an equilibrium between 5-coordinate and 6-coordinate species (Smulevich et al., 1988).

(ν_{10}), and 1570 cm^{-1} (ν_{19}) (Figure 7). H132A shows very similar bands at 1569 (ν_2), 1490 (ν_3) (Figure 6), 1627 (ν_{10}), and 1570 cm^{-1} (ν_{19}) (Figure 7). Since the histidine proximal ligation is maintained in His-132 mutants, the fifth ligand for these 5cHS species is the original histidine (Fe^{III}−His25). Thus, mutation of His-132 to an alanine or serine eliminates the coordination of the distal H_2O molecule. This large perturbation indicates that His-132 occupies a position close to the ligand binding site and plays a role in O_2 binding/activation in the distal heme pocket. This is probably the reason why His-132 is located in a highly conserved 24-amino acid sequence. The results described here imply that this domain forms the distal heme pocket, as suggested in our previous studies (Sun et al., 1994; Hernàndez et al., 1994).

DISCUSSION

The function of His-132 in HO-1, following unambiguous identification of His-25 as the proximal ligand (Sun et al., 1993, 1994; Takahashi et al., 1994a,b; Wilks et al., 1995), has been unclear. The conflicting nature of the data available on the H132A mutant (Ishikawa et al., 1992; Ito-Maki et al., 1995) has been resolved by the study of several purified His-132 hHO-1 mutant proteins. As shown here, the H132G and H132A mutants retain 40−50%, and the H132S mutant 20%, of the activity of wild-type hHO-1 (Table 1). The 5-fold increases in the K_m values, and the 10−50-fold increases in the heme dissociation constants (K_d), indicate that the mutants bind heme with a substantially lower affinity than the wild-type protein (Table 1). These results indicate that the distal histidine influences both substrate binding and turnover but, given the high level of activity of the Ala and Gly mutants, is not essential for catalytic activity.

The absorption spectra of the complexes of the His-132 hHO-1 mutants with ferric heme markedly differ from those of the wild-type hHO-1 complex. In contrast to the Soret maximum of the wild-type complex at 404 nm, the three mutants exhibit broad Soret peaks that extend into the region below 400 nm (Figure 3). Reduction of the mutant heme−hHO-1 complexes under a CO atmosphere generates ferrous−CO complexes with spectra similar to that of the wild-type hHO-1 complex. Passage of the wild-type hHO-1 ferrous−CO complex through a Sephadex G-25 column results in displacement of the CO by O_2 to give a stable ferrous−O_2 complex. In contrast, passage of the H132G and H132A heme−hHO-1 complexes through Sephadex G-25 results in the formation of transient ferrous−O_2 complexes that rapidly autoxidize to the resting ferric state (Figure 3A,B). Indeed, passage of the H132S heme−hHO-1 complex through Sephadex G-25 yields the resting ferric state without detectable formation of the ferrous−O_2 complex, presumably because the ferrous−O_2 complex autoxidizes too rapidly to be observed (Figure 3C).

Turnover of the wild-type heme−hHO-1 complex with cytochrome P450 reductase and NADPH under a partial CO atmosphere produces a shift in the Soret band from 404 to 418 nm as the FeCO complex is formed. Subsequent displacement of the CO by O_2 causes a shift of the Soret band back to 410 nm that is paralleled by a drop in its intensity as the heme is oxidized to biliverdin (Figure 4A). In contrast, no shift is seen in the Soret band when the mutant hHO-1−heme complexes are turned over with cytochrome P450 reductase and NADPH (Figure 4B−D). Despite the lack of spectroscopic evidence for the formation of either the ferrous−CO or −O_2 complexes under turnover conditions, the Soret band intensity decreases with all three mutants, and this decrease is accompanied, in the case of the H132G and H132A complexes, by small increases in the 640−680 nm absorbance characteristic of biliverdin formation (Figure 4). Extraction and HPLC analysis of the reaction products have confirmed that the major product formed in the reactions of the H132G and H132A mutants is biliverdin IXα. No biliverdin could be detected in the reaction of H132S hHO-1 under these conditions, presumably because the product was formed in too low a yield to be isolated. The absence of a shift in the Soret band during catalytic turnover of the mutants under a partial CO atmosphere, in conjunction with the evidence that an unstable ferrous−O_2 complex is actually formed when the mutant heme−hHO-1 complexes are reduced with dithionite, suggests that His-132 stabilizes the ferrous−O_2 complex in the wild-type protein. Loss of the His-132 interaction destabilizes the ferrous−O_2 complex with respect to autoxidation and presumably results in partial uncoupling of the consumption of NADPH from oxidation of the heme. His-132 does not appear, however, to function in an essential capacity in the catalysis of heme oxidation or in enforcing the regioselectivity of the reaction process. The effects of the His-132 mutations on the detailed stoichiometry of the reaction are under investigation.

We demonstrated earlier that H_2O_2 supports the heme oxygenase-catalyzed α-*meso*-hydroxylation of heme (Wilks & Ortiz de Montellano, 1993). In the presence of O_2, the α-*meso* hydroxylated heme is unstable and is converted by the enzyme to verdoheme. In the case of the His-132 hHO-1 mutants, addition of H_2O_2 (1−5 equiv) to the enzyme−heme complexes produces a slight decrease in the Soret absorbance, but there is no spectroscopic evidence for the formation of verdoheme (not shown). Furthermore, addition of pyridine to the mutant heme−protein complexes after reaction with H_2O_2 does not produce the distinctive spectrum of the verdoheme−pyridine complex that is obtained under the same conditions with the wild-type protein. The reaction of H_2O_2 with the heme−hHO-1 complex is thus completely dependent on the presence of His-132, whereas His-132 is not essential for the reaction supported by NADPH−cytochrome P450 reductase. This surprising mechanistic difference between the NADPH- and H_2O_2-dependent reactions suggests that the histidine may be required to deprotonate the peroxide and thus facilitate its binding to the iron atom. The normal NADPH-dependent reaction involves the binding of O_2 (which requires no deprotonation) to the ferrous enzyme.

Previous rRaman and EPR studies have shown that the proximal ligand in hHO-1 is His-25 (Sun et al., 1994; Ito-Maki et al., 1995). Key evidence in this regard was provided by the presence of the Fe−N_{His} stretching band at 216 cm^{-1} in the rRaman spectrum of the complex of heme with the wild-type, but not His-25, mutant (Sun et al., 1994). The rRaman spectrum of the ferrous His-132 hHO-1 mutants (Figure 5) exhibits the Fe−N_{His} band, in accord with the previous conclusion that His-25 is the proximal ligand. The wild-type heme−hHO-1 complex earlier was shown to be hexacoordinated, the two axial iron sites being occupied by His-25 and a water molecule (Sun et al., 1993; Takahashi et

al., 1994). The high-frequency region of the resonance Raman spectra (Figures 6 and 7) shows that the complexes of ferric heme with the H132A and H132S hHO-1 mutants are 5-coordinated. Since the proximal ligand remains intact in these mutants, as judged by the $Fe-N_{His}$ stretch at 216 cm^{-1}, the mutation of His-132 results in the loss of the H_2O molecule coordinated to the iron on the distal side of the heme. His-132 thus is important for stabilization of the H_2O that is bound in the ferric resting state. The loss of the water ligand and loss of the interactions with the distal side of the active site associated with water ligation are likely to be important determinations of the decreased affinities for the heme group that accompany the His-132 mutations (Table 1).

The results of the present study establish that His-132 is required for coordination of a water molecule to the iron in the resting state of the enzyme. This loss of water coordination, in addition to other possible changes in the active site of the His-132 mutants, presumably contributes to the decreased affinity of the enzyme for heme, its natural substrate. Furthermore, His-132 stabilizes the ferrous$-O_2$ complex but does not appear to play a critical role in catalytic steps beyond the formation of that complex. In the absence of His-132, catalytic turnover partitions between normal heme oxidation and uncoupling of NADPH consumption from heme oxidation due to autoxidation of the ferrous$-O_2$ complex. In contrast, His-132 is required for the H_2O_2-dependent oxidation of heme to verdoheme by hHO-1. The role of His-132 in stabilizing the distal water ligand and the ferrous$-O_2$ complex, and in activating H_2O_2 for catalytic turnover, argues that His-132 is located close to the iron on the distal side of the heme. Therefore, it is likely that other residues of the highly conserved 24-amino acid sequence that includes His-132 line the distal site cavity, some of which may be involved in the catalytic mechanism of the enzyme.

REFERENCES

Bonnett, R., & McDonagh, A. F. (1973) *J. Chem. Soc., Perkin Trans. 1*, 881−888.

Docherty, J. C., & Brown, S. B. (1984) *Biochem. J. 222*, 401−406.

Hernández, G., Wilks, A., Paolesse, R., Smith, K. M., Ortiz de Montellano, P. R., & La Mar, G. N. (1994) *Biochemistry 33*, 6631−6641.

Ishikawa, K., Sato, M., Ito, M., & Yoshida, T. (1992) *Biochem. Biophys. Res. Commun. 182*, 981−986.

Ito-Maki, M., Ishikawa, K., Matera, K. M., Sato, S., Ikeda-Saito, M., & Yoshida, T. (1995) *Arch. Biochem. Biophys. 317*, 253−258.

Loehr, T. M., & Sanders-Loehr, J. (1993) *Methods Enzymol. 226*, 431−470.

Maines, M. D. (1992a) *Heme Oxygenase: Clinical Applications and Functions*, pp 109−144, CRC Press, Boca Raton, FL.

Maines, M. D. (1992b) *Heme Oxygenase: Clinical Applications and Functions*, pp 203−266, CRC Press, Boca Raton, FL.

Maines, M. D., Trakshel, G. M., & Kutty, R. K. (1986) *J. Biol. Chem. 261*, 411−419.

Marks, G. S. (1994) *Cell. Mol. Biol. 40*, 863−870.

McCoubrey, W. K., & Maines, M. D. (1993) *Arch. Biochem. Biophys. 302*, 402−408.

Sambrook, J., Fritsch, E. F., & Maniatis, T. (1989) *Molecular Cloning: A Laboratory Manual*, Cold Spring Harbor Laboratory Press, Cold Spring Harbor, NY.

Smulevich, G., Mauro, J. M., Fishel, L. A., English, A. M., Kraut, J., & Spiro, T. G. (1988) *Biochemistry 27*, 5477−5485.

Stevens, C. F., & Wang, Y. (1993) *Nature 364*, 147−149.

Sun, J., Wilks, A., Ortiz de Montellano, P. R., & Loehr, T. M. (1993) *Biochemistry 32*, 14151−14157.

Sun, J., Loehr, T. M., Wilks, A., & Ortiz de Montellano, P. R. (1994) *Biochemistry 33*, 13734−13740.

Takahashi, S., Wang, J., Rousseau, D. L., Ishikawa, K., Yoshida, T., Host, J. R., & Ikeda-Saito, M. (1994a) *J. Biol. Chem. 269*, 1010−1014.

Takahashi, S., Wang, J., Rousseau, D. L., Ishikawa, K., Yoshida, T., Takeuchi, N., & Ikeda-Saito, M. (1994b) *Biochemistry 33*, 5531−5538.

Verma, A., Hirsch, D. J., Glatt, C. E., Ronnett, G. V., & Snyder, S. H. (1993) *Science 259*, 381−384.

Wilks, A., & Ortiz de Montellano, P. R. (1993) *J. Biol. Chem. 268*, 22357−22362.

Wilks, A., Black, S. M., Miller, W. L., & Ortiz de Montellano, P. R. (1995a) *Biochemistry 34*, 4421−4427.

Wilks, A., Sun, J., Loehr, T. M., & Ortiz de Montellano, P. R. (1995b) *J. Am. Chem. Soc. 117*, 2925−2926.

Yoshida, T., & Kikuchi, G. (1979) *J. Biol. Chem. 254*, 4487−4491.

Yoshida, T., Biro, P., Cohen, T., Müller, R. M., & Shibahara, S. (1988) *Eur. J. Biochem. 171*, 457−461.

Yoshida, T., Ishikawa, K., & Sato, M. (1991) *Eur. J. Biochem. 199*, 729−733.

BI952405F